Tribology Letters, Vol. 18, No. 4, April 2005 (© 2005)
DOI: 10.1007/s11249-005-3607-8


# Ultralow-friction and wear properties of IF-$WS_2$ under boundary lubrication

L. Joly-Pottuz[a,*], F. Dassenoy[a], M. Belin[a], B. Vacher[a], J.M. Martin[a] and N. Fleischer[b]

[a]Ecole Centrale de Lyon, LTDS, bât H10, 36 avenue Guy de Collongue 69134, Ecully, France
[b]NanoMaterials, Ltd, Weizmann Science Park, 2 Holtzman Street, Rehovot 76124, Israel

Received 31 October 2004; accepted 2 January 2005

Tested in boundary lubrication, inorganic fullerene-like $WS_2$ nanoparticles used as additives in oil present interesting friction reducing and anti-wear properties. A dispersion with only 1 wt% of particles leads, from a contact pressure of 0.83 GPa, to a drastic decrease of the friction coefficient below 0.04 and to very low wear. High resolution transmission electron microscopy (HRTEM), Scanning Electron Microscopy (SEM), X-ray diffraction (XRD), Raman Spectroscopy and video imaging were used to explain the lubrication mechanisms. A structural modification of fullerene-like nanoparticles into sheets during the friction test was evidenced to be the main effect at the origin of these properties.

**KEY WORDS:** inorganic fullerene-like $WS_2$ nanoparticles, boundary lubrication, friction, tribology, Raman spectroscopy, X-ray diffraction, transmission electron microscopy, video-imaging

## 1. Introduction

The lubrication mechanisms of the most used friction reducing and anti-wear lubricant additives (MoDTC and ZnDTP) have widely been studied in the past [1,2]. They are based on chemical reaction which occurs in the contact area during the friction, leading to the formation of active products. Thus, friction reducing properties of molybdenum dithiocarbamate (MoDTC) are due to the formation of $MoS_2$ sheets in the contact area, induced by high temperature and pressure. This additive is however at the origin of sulphur containing reaction products (radicals) which are very harmful for the environment [2]. The research of new friction reducing and anti-wear lubricant additives as efficient as these additives, but much less polluting for the environment, constitutes actually a new challenge in tribology.

By analogy to carbon fullerenes, Tenne *et al.* have synthesised inorganic fullerene-like nanoparticles of metal dichalcogenides (IF-$MX_2$) [3]. Because of their unique morphology, these nanoparticles were supposed to present interesting tribological properties. Their nanometric size could allow them to enter easily the contact area and to be directly active. Moreover, their spherical shape (without dangling bonds) confers them a chemical inertness; thus these particles do not adhere to surfaces like platelets of the 2H polytype. Their hollow structure confers them a high elasticity allowing one to suppose that these particles can roll in the contact area. These materials have recently motivated extensive research on their tribological properties. If carbon based fullerenes do not present exceptional tribological properties [4,5], it has been shown that inorganic fullerene-like particles significantly improve the tribological performances of a fluid when added as additives [6]. Cizaire *et al.* [7] have recently tested IF-$MoS_2$ nanoparticles as additives in lubricated contact under high contact pressure. A low friction coefficient has been reached and the correlation between tribological properties of IF-$MoS_2$ and its structure has been established. An exfoliation of the external sheets of $MoS_2$ fullerene-like nanoparticles was found to occur during the friction test. This mechanism illustrates the advantage of the use of nanoparticles instead of organic compounds. Both produce $MoS_2$ sheets directly active in the contact area, but in the case of fullerene-like nanoparticles this occurs without chemical reaction.

Although many studies have also been performed with $WS_2$, relatively little has been carried out under boundary lubrication. The more important study on this material has been performed by Rapoport *et al.* [8]. They have tested the tribological behaviour of these particles as additives in oil and grease under mixed lubrication but also as enhancements in polymer, metal coatings and impregnated into self-lubricating sintered porous metal parts [9,10]. In all cases the tribological behaviour was improved. Like for the IF-$MoS_2$, they showed that exfoliation of the IF onion and transfer of $WS_2$ sheets onto the two surfaces in contact is at the origin of this improvement. Rapoport *et al.* have also compared tribological properties of IF-$WS_2$, 2H-$WS_2$ and 2H-$MoS_2$ used as additives to lubricants under mixed lubrication and have shown that the fullerene-like

*To whom correspondence should be addressed.
E-mail: lucile.joly-pottuz@ec-lyon.fr

nanoparticles contribute to reduce much more the friction than the layered structure [11]. They have attributed this result to the size of the particles in the contact area which decreases of the fraction of straight asperities [12].

In this work IF-$WS_2$ was tested under boundary lubrication as an additive in a synthetic base oil, a polyalphaolefin (PAO). The objective of this work is to test the efficiency of these particles in severe conditions of friction and to investigate the influence of two main parameters, which are the concentration and the contact pressure, on the tribological behaviour of the dispersion. This is of major importance to understand which mechanisms occur in the contact area. To understand the mechanisms involved in the contact area, a set of experimental techniques was used. The structural characterisation of the fullerene-like nanoparticles before and after friction was performed by Transmission electron microscopy (TEM), X-ray diffraction (XRD) and Raman spectroscopy. These techniques are very powerful to observe structural changes induced by the friction process. Scanning electron microscopy (SEM) was also performed on the two antagonist surfaces after friction. The correlation between tribological properties and structural modification were able to be established with the application of these techniques.

## 2. Experimental section

### 2.1. Synthesis

A special fluidised bed reactor (FBR) made of quartz glass was constructed for these experiments [13]. In this reactor $WO_3$ nanoparticles are fed (40–70 mg/min) from the top. Auxiliary $N_2$ gas flow (60 mL/min) facilitates the dropping of the powder into the reactor. A mixture of gases consisting of $H_2S$ (5–12 mL/min) and $H_2$ (5%)/$N_2$ (95%) (60–120 mL/min) flows from below keeping the powder fluidised within the reactor. The powder is collected on a porous filter. A temperature profile of between 800 and 840 °C is maintained along the 60-cm long reactor. Typically the reaction is run overnight with some 40–70 g of powder collected on the porous filter. The typical size distribution of the fullerene-like nanoparticles is between 60–150 nm (and even some larger particles are present). The median size of the nanoparticles used in these tests was 140 nm.

### 2.2. Tribological conditions

IF-$WS_2$ nanoparticles were tested in a lubricated contact using a pin-on-flat tribometer, with both surfaces made of AISI 52100 steel and polished with a 1 $\mu$m diamond solution. *In situ* video imaging and Raman spectroscopy of the sliding contact regions were carried out by replacing the steel flat by a sapphire flat.

Tribological tests were performed in ambient air (30–35 RH) and ambient temperature (25 °C), with a sliding velocity of 2.5 mm/s and a stroke length of 2.5 mm. Several diameters of pin were used to test a range of contact pressures from 0.33 to 1.72 GPa. The pin diameter was adjusted in function in order to achieve the desired contact pressure: 12 mm from 0.33 to 0.52 GPa, 6 mm from 0.66 to 1.12 GPa and 4.5 mm for 1.72 GPa. With these conditions, experiments are performed under boundary lubrication. Two droplets of lubricant were deposited on the flat just before starting the experiments. The lubricant was a dispersion of IF-$WS_2$, at different concentrations, in a synthetic base oil, a polyalphaolefin (PAO). No dispersant was used. The dispersion IF/PAO was made by using an ultrasonic bath and was optically stable for several hours.

### 2.3. Analytical tools

Specimens for TEM studies were prepared by slow evaporation of a drop of suitably diluted particles containing solutions deposited on perforated carbon-covered copper grids. The observations were carried out on a LEO 912 instrument operating at 200 kV accelerating voltage for conventional TEM studies and on a JEOL 2010 FEG electron microscope operating at 200 kV (with a point resolution of 0.2 nm) for the HRTEM. The size distribution of the particles was determined through numerical analysis of TEM low magnification images. Histogram of the size distribution included the measurement of about 200 particles, and was reproduced in different regions of the sample. HRTEM experiments were used to determine the fine structure of the wear debris particles. The angles between the different sets of fringes and the different fringes' spacing were measured from numerical diffractograms (Fourier transforms) of HRTEM images and compared with the angles and distances of the atomic planes of different phases.

X-ray patterns were obtained with a Guinier powder diffractometer (HUBER), set to the 45° transmission position. A Johansson type germanium monochromator produces a focussed monochromatic Cu-K$\alpha$1 primary beam ($\lambda = 0.15406$ nm). Samples were prepared by the following process: wear particles were collected by cleaning the flat with pure heptane. Several drops of the solution were then deposited onto a 3 $\mu$m thick polyethylene foil. XRD patterns were measured with high resolution in the step-scanning mode with a narrow receiving slit (0.125°) in the range 5°–30°. All scans were recorded at room temperature and under ambient atmosphere. The background-corrected patterns were plotted versus the angle theta.

Raman spectra were recorded in back scattering configuration using a Labram HR 800 microspectrometer manufactered by Jobin Yvon. Excitation wavelength of 632.8 nm was produced by a He/Ne laser source capable of supplying 20 mW power. A density filter was used to reduce the incident power close to 50 $\mu$W. The excitation laser power was selected carefully to avoid heating effects on spectra. Several locations of each sample surface were probed to ensure reproducibility of the data. The instrumental resolution was 1 $cm^{-1}$ for the 1800 g/mm grating. The calibration was performed with silicon semiconductor at 520.7 $cm^{-1}$.

Scanning Electron Microscopy was used to observe the pin after friction and to characterise the tribofilm on the surface. Observations were performed using a FEI XL 30 ESEM FEG operating in vacuum and with an accelerating voltage of 10 kV.

## 3. Characterisation before friction

In order to fully understand the tribological properties of IF-$WS_2$, a precise structural characterisation of this material before friction is necessary. Indeed, size and structural defects like dislocations can have an influence on their tribological properties. TEM micrographs (figure 1(a) and (b)) show that the fullerene-like nanoparticles are nearly spherical and form a nested shape structure. A size distribution made by TEM on 200 particles indicates that their diameter is between 80 and 200 nm (figure (c)). The mean diameter is close to 140 nm.

Figure 2 shows the wide-angle X-ray scattering pattern (WAXS) of the as-synthesised particles compared to that of the pure hexagonal layered structure material. Undoubtedly the IF-$WS_2$ particles adopt the same crystal structure than the 2H-$WS_2$. Nevertheless, due to the small size of the particles and to their nested shape structure, some of the peaks are much less resolved. Thus from the spectra, it is clear that the IF-$WS_2$ shows strong lateral disorder with the typical extreme broadening of all h0l type peaks. These peaks appear only if 3D ordering exists. An expansion of 1% of the c parameter (determined from the 002 peak) in the IF-$WS_2$ in comparison to the 2H-$WS_2$ has been observed. It is well known from graphite for example that the c-parameter must increase with increasing lateral disorder (loss of 3D order); this is the case in carbon fullerenes materials and nanotubes [14,15]. The lattice expansion was ascribed to strain relief in the folded structure. This feature has also been observed for other nested shape structures [13,16]. The observed (*hk*0) diffraction peaks show a asymmetric line shape, which result from stacking disorder.

IF-$WS_2$ and 2H-$WS_2$ were characterised by Raman spectroscopy. Both spectra (figures 3(a) and (b)) indicate the presence of two strong peaks at 352 and 421 $cm^{-1}$ which correspond to the $E^1_{2g}$ and $A_{1g}$ modes, respectively. The peak at 421 $cm^{-1}$ is slightly splitted for 2H-$WS_2$. This split seems to be more pronounced for IF-$WS_2$. This is caused by a contribution at 416 $cm^{-1}$ which could be due to a second order Raman effect [17].

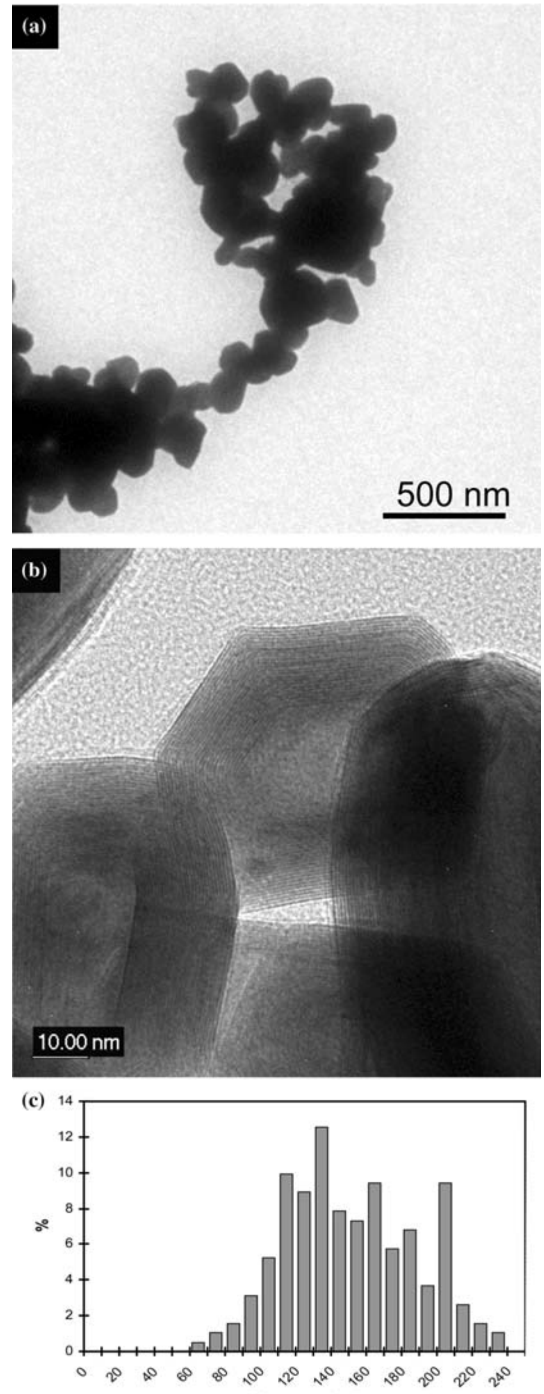


Figure 1. (a) and (b) TEM images of IF-$WS_2$, (c) size distribution of IF-$WS_2$.

## 4. Tribological results

In order to find the concentration giving the best tribological behaviour, several dispersions of IF were tested with a contact pressure of 1.12 GPa: 0.1, 0.5, 1 and 2 wt%. Figure 4(a) shows the influence of the fullerene-like nanoparticles concentration on the friction coefficient. The results show that the addition of only

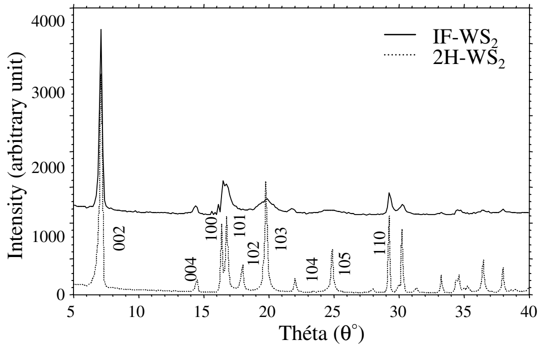


Figure 2. XRD patterns of the pristine material (full line) and pure hexagonal $WS_2$ (dotted line).

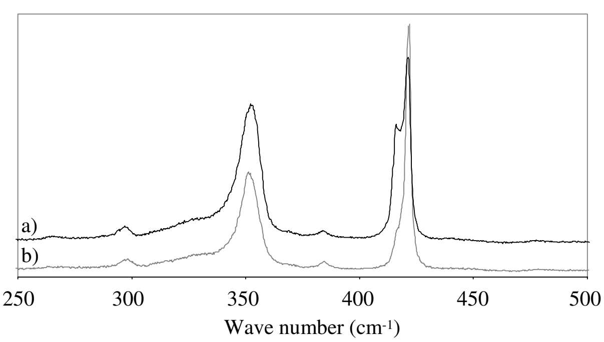


Figure 3. Raman spectra of: (a) IF-$WS_2$ and (b) 2H-$WS_2$.

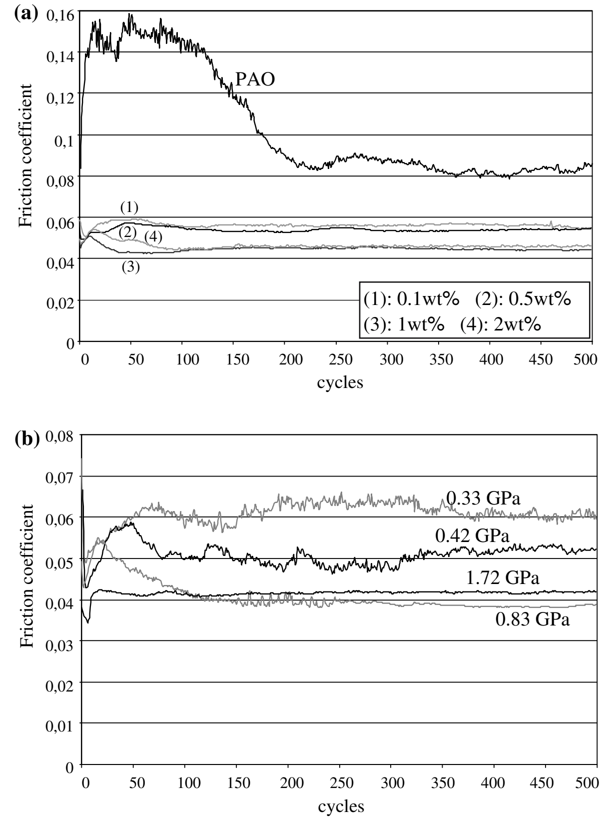


Figure 4. Evolution of friction coefficient in a lubricated contact: (a) influence of IF-$WS_2$ concentration in PAO—contact pressure of 1.12 GPa, (b) effect of contact pressure for 1 wt% IF-$WS_2$ in PAO.

0.1 wt% of fullerene-like nanoparticles in the base oil is sufficient to strongly reduce the friction coefficient in comparison with pure PAO. Moreover, the friction coefficient is low from the very beginning of the experiment (0.055) and is then pretty stable throughout the test which is not the case with pure PAO. Then the higher the concentration, the lower the friction coefficient is. It stabilises around 0.04 for 1 wt% of fullerene-like nanoparticles. A further increase of the fullerene-like nanoparticles concentration does not improve friction.

A study of the effect of the contact pressure (from 0.33 to 1.72 GPa) on the tribological properties of fullerene-like nanoparticles was performed with the optimal concentration (1 wt%). For a better understanding of the graph, only the most important results are summarised in figure 4(b). From 0.33 up to 0.83 GPa, the higher the contact pressure, the lower the friction coefficient is. For this value the friction coefficient is below 0.04. A further increase of the pressure does not affect really the friction coefficient which can be considered stable (around 0.04). These results let one suppose a pressure-induced structural modification of the fullerene-like nanoparticles during friction test.

Observations of wear scar diameters on the pin are very useful to determine the anti-wear properties of an additive. They were measured for each pressure (see table 1). Each of them is very close to the calculated Hertz diameter. Compared to the pure PAO these diameters are much less important. This comparison clearly shows the anti-wear properties of the fullerene-like nanoparticles. The aspect of the wear scar is worth observing since it can provide useful information for the understanding of the good tribological properties of the material. Some of them are reported on figure 5 (PAO, and 3 dispersions: PAO + fullerene-like nanoparticles). Whatever the pressure, the general aspect of the wear scar is the same and is composed of a blue circular tribofilm in the middle of the pin while a brown crown delimits the scar. From these observations, we can suppose that the tribofilm in the middle of the scar is formed during the friction while the crown could be due to agglomerates of fullerene-like nanoparticles which stick to the pin and which are unable to enter the contact area due to their large size. To confirm this hypothesis, video imaging was performed with the following experimental conditions: 1 wt% of IF-$WS_2$, contact pressure of 1.12 GPa. Figure 6 shows a sequence of captured image at $t=0$ s, $t=120$ s, $t=180$ s, $t=330$ s and at the end of the test. This sequence shows that the formation of the tribofilm, observed on the pictures of the figure 5, is progressive and continues all throughout the test. The formation of agglomerates is also visible all

Table 1.
Wear scar diameters obtained with a concentration of 1 wt% and the corresponding calculated Hertz diameter for different contact pressures (from 0.33 to 1.72 GPa).

| Contact pressure (GPa) | Pin diameter (mm) | Calculated Hertz diameter ($\mu$m) | Wear scar diameter ($\mu$m) | Wear scar diameter with pure PAO ($\mu$m) |
|---|---|---|---|---|
| 0.33 | 12 | 54 | 65 | 85 |
| 0.42 | 12 | 68 | 80 | 115 |
| 0.52 | 12 | 86 | 95 | 150 |
| 0.66 | 6 | 54 | 75 | 115 |
| 0.83 | 6 | 68 | 86 | 170 |
| 1.12 | 6 | 92 | 100 | 175 |
| 1.42 | 6 | 116 | 120 | 180 |
| 1.72 | 4.5 | 106 | 115 | 150 |

Values of wear scar diameter obtained with pure oil are also mentioned.

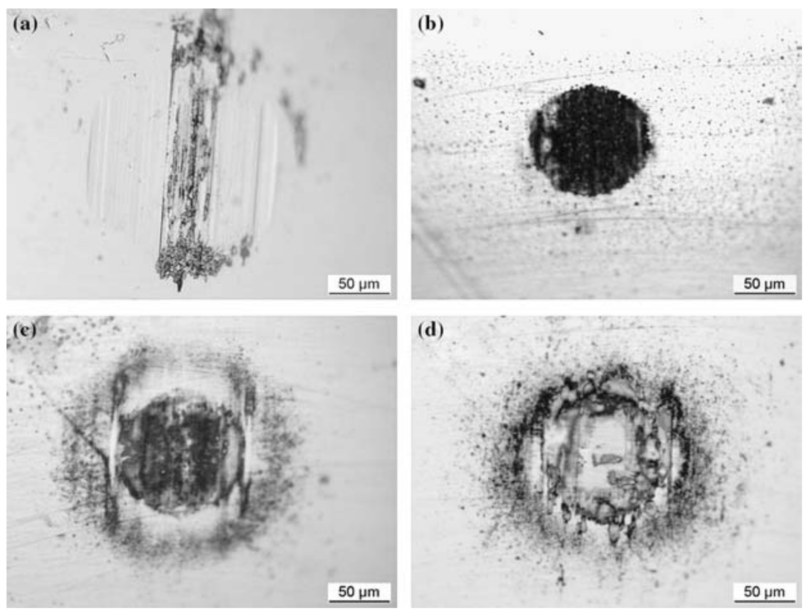


Figure 5. Wear tracks on pin for: (a) PAO, (b) PAO + 0.1 wt% IF-$WS_2$, (c) PAO + 0.5 wt% IF-$WS_2$, (d) PAO + 1 wt% IF-$WS_2$.

around the contact area. The supply of the contact area during the test is difficult to discuss since with this machine only the observation of agglomerates of particles is possible. Nevertheless the very low friction coefficient reached from the beginning of the test and its stability let suppose that first the fullerene-like nanoparticles are already present and therefore active at $t = 0$ s and second, that the supply in particles occurs continuously. From this observation a first assumption can be made to explain the reduction of the friction and wear rate on the contacting surfaces. We can effectively suppose that these agglomerates of particles increase the load-carrying-capacity of the particles already present in the contact area.

## 5. Characterisation after friction

TEM observations of wear particles collected on the pin after the friction tests performed with the optimal conditions (1 wt% and 1.12 GPa) show the presence of $WS_2$ sheets (figure 7). Since these sheets are not observed in the pristine material, this indicates a structural modification of fullerene-like nanoparticles into $WS_2$ sheets. This lubrication mechanism has already been observed with $MoS_2$ fullerene-like nanoparticles by Cizaire *et al*. [7].

HRTEM observation of these sheets in very thin regions confirms the hexagonal structure of the sheets. In several sheets, we can also observed Moiré patterns in some areas indicating the presence of superimposed sheets with a rotational angle between them (figure 7). Misfit angle can be calculated by FFT of the HRTEM image. Figure 7 indicates an angle of 10° between two sheets and another of 30° between one of them and a third one. Near 10°, there are still regions of atomic coincidence between the planes. But, this coincidence disappears with a rotation angle of 30°, allowing a more easy shear. It has been demonstrated that the [2110] orientation can be very interesting to monitor changes in the atomic configuration because it permits to see the

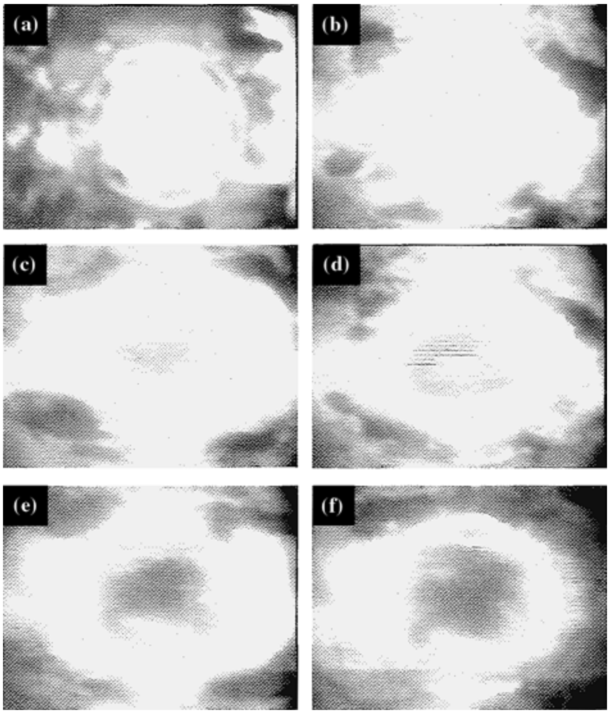


Figure 6. Captured images at different times during a friction test (1 wt%, 0.83 GPa): (a) 0 s, (b) 60 s, (c) 120 s, (d) 180 s, (e) 330 s and (f) 480 s.

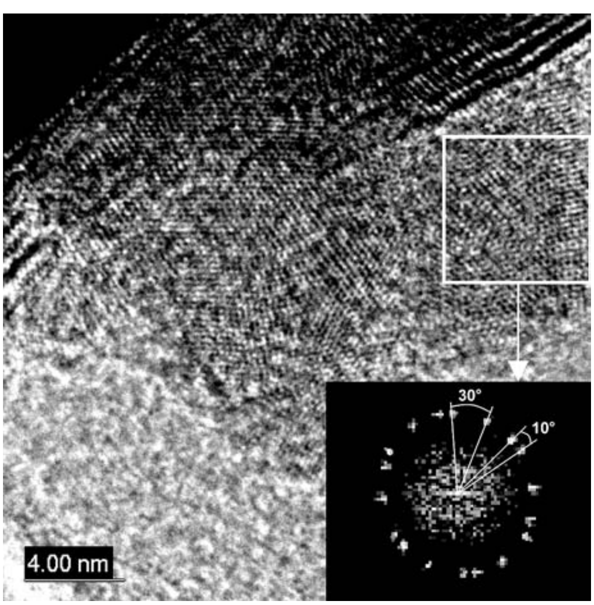


Figure 7. HRTEM image of wear debris collected on the wear scar with the corresponding calculated diffractogram.

alternate chevron-like structure [18]. But, in the case of wear particles, crystallites reorient with their basal plane parallel to the sliding direction. This mechanism has already been observed by Martin *et al.* in the case of $MoS_2$ coatings and the authors attribute the superlubricity of $MoS_2$ to this phenomenon [19,20].

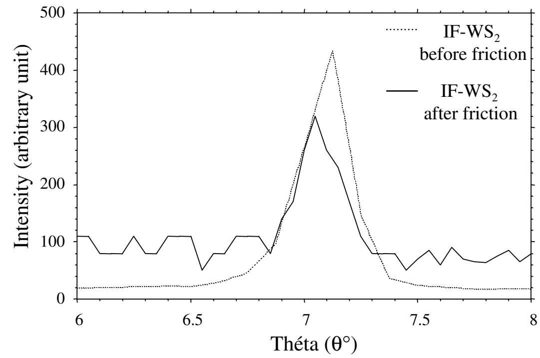


Figure 8. XRD patterns of the pristine material (full line) and wear particles collected after friction (dotted line).

Due to the small amount of collected wear particles, the quality of the XRD spectra recorded after the friction test is poor. Only the most intensive peak of diffraction (002) is meaningful (figure 8). The position of this peak was compared to that of the as-synthesised $IF\text{-}WS_2$. A new expansion of the c-parameter (+1%) in the structure of the wear particles in comparison with the as-synthesised particles indicates that after friction the lateral disorder increases even more, thus inducing a further increase in the mean *c*-spacing between the $WS_2$ planes.

Raman characterisation was performed both on the tribofilm formed on the pin and inside the wear scar on the flat. The spectra were compared with that obtained from $IF\text{-}WS_2$ before friction (figure 9). The shape of three spectra is very similar. This confirms that there is a transfer of matter both on flat and pin during the friction test. Nevertheless, it is difficult from Raman data to discuss an eventual structural or morphological modification of the fullerene-like nanoparticles. Several studies have shown that resonance Raman spectra of the fullerene-like materials show a close correspondence to the corresponding spectra for the 2H single-crystal system [21].

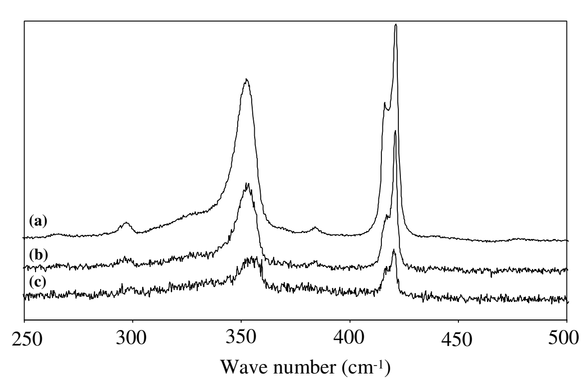


Figure 9. Comparison of Raman spectra obtained from: (a) $IF\text{-}WS_2$, (b) tribofilm on the flat, (c) tribofilm on the pin.

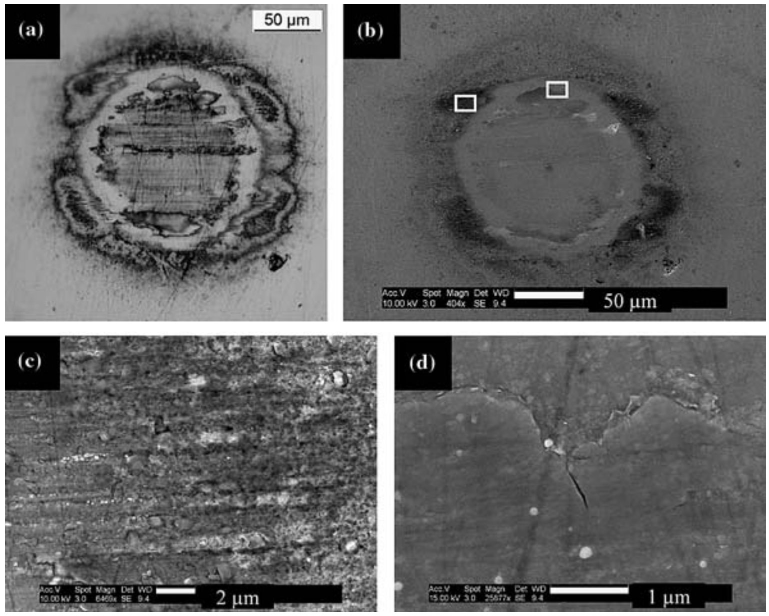


Figure 10. (a) optical image of the wear track on pin for 1%wt IF-$WS_2$. SEM images: (b) general view—left frame corresponds to figure (c) and right frame to figure (d), (c) view of the brown crown, (d) film observed inside the wear track.

SEM characterisations were performed in the wear scar of the pin (figure 10). Contrary to the optical image (figure 10(a)) a difference of contrast can been observed between the crown and the tribofilm formed on the wear scar (figure 10(b)). Figure 10(c) and (d) shows an enlargement of these two areas. A difference of texture can be observed. The roughness of the layer seems to be more important in figure 10(c) than in 10(d). This is consistent with a possible agglomeration of particles all around the contact area which therefore do not enter the contact and are not structurally modified, but also with the formation of coating film in the contact zone. Furthermore, this tribofilm seems to be quite thick.

## 6. Discussion

In this work it has been shown that when submitted to a certain critical pressure, very low friction coefficient can be reach under boundary lubrication, when only few percent or less of IF-$WS_2$ are added to a synthetic base oil. At the same time, the anti-wear properties of this dispersion have been shown. Information collected from the different chracterisation techniques used for this work allow one to make hypotheses about the origin of these properties.

It has clearly been shown that during the friction test, particles of IF-$WS_2$ which enter the contact progressively transform into h-$WS_2$ sheets. They are found in the wear debris mixed with some fullerene (intact and crushed) but also deposited on the two antagonist surfaces leading to a thin tribofilm which adheres on the metal substrates. The presence of $WS_2$ in the wear scar is furthermore confirmed by Raman. The low friction and the low wear on the two surfaces can be conferred by both a progressive delamination of the IF-$WS_2$ particles supplying the contact in lubricating IF-$WS_2$ sheets and by the gradual detachment from the surface of these particles free to roll and/or slide in the contact area. The delamination of the particles during the friction test leads nevertheless to the formation of dangling bonds like in the layered material. However in this case the appearance of dangling bonds is less problematic since first the delamination involves only few layers and second according to Schwarz *et al.* the delamination may occur under adhering conditions with the substrates which minimises the negative effects of the dangling bonds whose density remains low [22]. Our results are in agreement with those obtained by Golan *et al.* who have visualised by multiple beam interferometry (MBI) the behaviour of additive particles of IF-$WS_2$ confined and sheared between two mica surfaces [23]. Layer by layer exfoliation of the IF-$WS_2$ during shear was observed but no evidence for a "rolling friction". A strong adhesion of the IF-$WS_2$ to the mica was shown.

From our results, it has also been shown that the higher the contact pressure, the lower the friction coefficient is. This result confirms our hypothesis that a critical pressure must be reach to sufficiently delaminate the IF-particles and therefore optimise the decrease of the friction coefficient. If this critical pressure is not reached, the decrease of the friction coefficient is less important. Thus for 0.33 GPa the small decrease of the friction coefficient is certainly due to a rolling or sliding effect of the particles without delamination. The anti-wear properties of the IF-$WS_2$ are less sensitive to the load imposed during the test. Even at low pressure,

$IF-WS_2$ present good anti-wear properties. The particles present between the two surfaces avoid the contact between straight asperities [12].

The behaviour of these inorganic fullerene-like nanoparticles is finally very similar to that observed with other IF nanoparticles tested also as additives in a lubricating fluid. Thus, Cizaire *et al.* [7] have also reported such behaviour for $IF-MoS_2$ tested in similar conditions. The test was performed for only one contact pressure of 1.1 GPa but a coefficient close to 0.05 was reached. Flattened particles mixed with $h-MoS_2$ sheets were observed by TEM. Similar behaviour has also been observed by Joly-Pottuz *et al.* with Mo–S–I nanowires dispersed in PAO [24]. Dismantling of nanowires in $h-MoS_2$ sheets was proved thanks to Raman and XRD experiments. However in this case, the life time of the tribofilm deposited on the surfaces was much less significant than that obtained with $IF-MoS_2$ or $IF-WS_2$ and an increase of the friction coefficient was observed after a number of cycles depending of the contact pressure.

If we compare more in detail the results obtained by Cizaire *et al.* to ours, we can nevertheless note that the mean diameter of the $WS_2$ fullerene-like nanoparticles is approximately three times larger than that of the $MoS_2$ fullerene-like nanoparticles. This is of major importance since with regarding the $WS_2$ particles, we have clearly observed the presence of a brown crown around the wear scar meaning that the larger particles can not directly enter the contact area but contribute nevertheless to produce an additional bearing effect which probably contributes to the decrease of the friction. This effect could explain that with $IF-WS_2$ the friction coefficient is 20% lower than with $IF-MoS_2$.

Schwarz *et al.* have investigated theoretically the effect of adhesion, pressure and shear flow on the deformation and mechanical stability of hollow nanoparticles of spherical shape [22]. This theoretical understanding is of major importance to understand the tribological properties determined experimentally. They have shown that in friction experiment with IF-fullerene-like nanoparticles, the delamination is caused by the pressure but that it may occur under adhering conditions. Their study showed also that two parameters should be well controlled to optimise the tribological properties of the fullerene-like nanoparticles: the ratio of radius to thickness and the concentration of defects. The role of the size of the particles has already been discussed. The role of the defects in the particles has not yet been explored. However, the XRD experiments have shown that the particles were probably not well crystallised and the broadening of some peaks indicate a lateral disorder and the presence of stacking faults.

HRTEM is nevertheless a very useful technique to determine stacking faults in layered structure like $WS_2$ [18]. A misfit angle has been observed between the $WS_2$ sheets, allowing a more easily shear between them. This could also explain the very low friction coefficient observed in the case of the $WS_2$ fullerene-like nanoparticles in contrast to the $MoS_2$.

## 7. Conclusion

A very low friction coefficient and a low wear have been obtained with $IF-WS_2$ used as additives in oil and tested under boundary lubrication. From the characterisation performed after friction, several phenomena have been proposed to explain these friction reducing properties: fullerene-like nanoparticles delamination, formation of tribofilm made of $WS_2$ sheets on the surfaces, superlubricity of the sheets and probably a rolling/sliding effect of the particles. A combination of all these effects can explain the very good tribological properties of the fullerene-like nanoparticles and especially of $IF-WS_2$.

## Acknowledgments

The authors gratefully thank Dr. W. Vogel from the Fachhochschule Brandenburg (Germany) for X-ray diffraction measurements and fruitful discussions and G. Montagnac from the Ecole Normale Supérieure of Lyon for his support for the Raman spectroscopy experiments.

## References

[1] J.M. Martin, Tribol. Lett. 6 (1999) 1.
[2] C. Grossiord, K. Varlot, J.M. Martin, T. Le-Mogne, C. Esnouf and C. Inoue, Tribol. Int. 31 (1998) 737.
[3] R. Tenne, M. Homyonfer and Y. Feldman, Chem. Mater. 10 (1998) 3225.
[4] U.D. Schwarz, O. Zwörner, P. Köster and R. Wiesendanger, Phys. Rev. B 56 (1997) 6987.
[5] L. Seunghwan, S. Young-Seok, T.R. Lee and S.S. Perry, Thin Solid Films 358 (2000) 152.
[6] L Rapoport, Y. Bilik, Y. Feldman, M. Homyonfer, S.R. Cohen and R. Tenne, Nature 387 (1997) 791.
[7] L. Cizaire, B. Vacher, T. Le-Mogne, J.M. Martin, L. Rapoport, A. Margolin and R. Tenne, Surf. Coat. Technol. 160 (2002) 282.
[8] L. Rapoport, N. Fleischer and R. Tenne, Advanced Materials 15 (2003) 651.
[9] L. Rapoport, O. Nepomnyashchy, A. Verdyan, R. Popovitz-Biro, Y. Volovik, B. Ittah and R. Tenne, Adv. Eng. Mater. 6 (2004) 44.
[10] L. Rapoport, M. Lvovsky, I. Lapsker, W. Leshchinsky, Y. Volovik, Y. Feldman and R. Tenne, Wear 249 (2001) 150.
[11] L. Rapoport, Y. Feldman, M. Homyonfer, H. Cohen, J. Sloan, J.L. Hutchison and R. Tenne, Wear 225 (1999) 975.
[12] L. Rapoport, V. Leschchinsky, I. Lapsker, Y. Volovik, O. Nepomnyashchy, M. Lvovsky, R. Popovitz-Biro and R. Tenne, Wear 255 (2003) 785.
[13] Y. Feldman, Wasserman, D.J. Srolovitz and R. Tenne, Science 267 (1995) 222.
[14] Y. Saito, T. Yoshikawa, S. Bandow, M. Tomita and T. Hayashi, Phys. Rev. B 48 (1993) 1907.
[15] Y. Yosida, Appl. Phys. Lett. 64 (1994) 3048.
[16] L. Cizaire, J.M. Martin, F. Dassenoy, B. Vacher, C. Geantet and R. Tenne, Appl. Surf. Sci. Submitted.

[17] C. Sourisseau, F. Cruege, M. Fouassier and M. Alba, Chem. Phys. 150 (1991) 281.
[18] T. Isshiki, K. Nishio, I. Aoyagi, Y. Yabuuchi, N. Takahashi, H. Saijo and M. Shiojiri, Wear 170 (1993) 55.
[19] J.M. Martin, C. Donnet, T. Le-Mogne and T. Epicier, Phys. Rev. B 48 (1993) 10583.
[20] J.M. Martin, H. Pascal, C. Donnet, T. Le-Mogne, J.L. Loubet and T. Epicier, Surf. Coat. Technol. 68/69 (1994) 427.
[21] G.L. Frey, R. Tenne, M.J. Matthews, M.S. Dresselhaus and G. Dresselhaus, J. Mater. Res. 13 (1998) 2412.
[22] U.S. Schwarz, S. Komura and S.A. Safran, Europhys. Lett. 50 (2000) 762.
[23] Y. Golan, C. Drummond, J. Israelachvili and R. Tenne, Wear 245 (2000) 190.
[24] L. Joly-Pottuz, F. Dassenoy, J.M. Martin, D. Vrbanic, A. Mrzel, D. Mihailovic, W. Vogel and G. Montagnac, Tribol. Lett. 18(3) (2005) 383.